Ceramic membranes originated from cost-effective and abundant natural minerals and industrial wastes for broad applications – a review

Linquan Sun[a,b], Ziyi Wang[c,†], Baoyu Gao[b,*]

[a]*China Resources Environmental Protection Development Limited, Shenzhen 518001, China, Tel. +86-18682155423;*
email: myth619@163.com (L.Q. Sun)
[b]*Shandong University, Jinan 250100, China, Tel. +86 531-88366771; bygao@sdu.edu.com (B.Y. Gao)*
[c]*Pingan International Smart City Technology Co., Ltd., Pingan Group, Shenzhen 410083, China, Tel. +86-15710791239;*
email: 15710791239@139.com (Z.Y. Wang)

ABSTRACT

The wide application of ceramic membranes in nowadays can be rationalized by their intrinsic properties, notably in terms of thermal and chemical stability and high mechanical strength. Compared to the conventional metal oxide materials, this article summarized comprehensively the natural minerals and industrial wastes, which are in abundance and need lower firing temperature, for the ceramic membrane fabrication as the raw materials. These cost-effective ceramic membranes prepared from clay, silty marls, kaolin, zeolite, bauxite, quartz sands, bentonite, cordierite, apatite, perovskite, coal fly ash, coal gangue, blast furnace slag, rice husk ash, pozzolan, etc. have emphasized the remarkable cost reduction and been broadly applicable to a variety of fields like removal of solid, dye, ion, heavy metal, oily wastewater treatment, juice clarification, seawater desalination, sterilization, hydrogen separation, oxygen permeation, CO_2 adsorption and separation, membrane catalysis, etc. The cost of these natural minerals and industrial wastes based ceramic membrane was estimated several times cheaper than the conventional oxide ceramic membrane. This review encouraged a more economically viable and environmentally sustainable strategy, not only giving a new and facile insight for waste management but also endow a possibility of high-valued recycling.

Keywords: Ceramic membrane; Natural minerals; Industrial wastes; Cost effective

1. Introduction

Membrane technologies were usually considered as a common disposal strategy for wastewater treatment and have proven to be beneficial in saving water consumption and costs. The penetrating, physical and chemical performances are thought to be the critical factors influenced membrane performances, in which penetrating performances including water flux, molecular weight cut-off, rejection rate, recovery rate, porosity, pore size distribution, mean pore size, maximum pore size, etc., physical performances including membrane shape, thickness, outer diameter, inner diameter, tensile strength, flexural strength, breaking elongation, surface charge, zeta potential, contact angle, thermal resistance, etc., chemical performances including chemical stability, antifouling property, corrosion resistance, etc. The penetrating performance of the membrane determined the amount, purity, as well as sensitivity of the product. The excellent physical and chemical performances were valuable for the application in a harsh environment. For example, temperature tolerance of the membrane in the membrane distillation process provided more practical opportunities for heat recovery, which could significantly further raise overall system efficiency [10]. The definitions of major properties are listed in Table 1.

---

* Corresponding author.

†Co-first author.

Table 1
Definitions of major properties

Type	Properties	Definition	Reference
Penetrating performance	Water flux	Product of inundation depth, the width of the channel and depth-averaged current velocity	[1]
	Molecular weight cut-off	Lowest molecular weight at which greater than 90% of a solute with a known molecular weight is retained by the membrane	[2]
	Recovery rate	Permeate flow rate divided by the membrane feed flow rate	[3]
	Porosity	Ratio of the pore volume to the whole nominal volume of a porous body, and is generally expressed as either a percentage or a decimal	[4]
Physical performance	Tensile strength	Level of the elastic tensile stress reached when the maximum value of stress is reached at the location of the fracture	[5]
	Flexural strength	Maximum stress at the outermost fiber on either the compression or tension side of the specimen	[6]
	Breaking elongation	Percentage increase in length when the yarn breaks due to a tensile force applied along the main yarn axis	[7]
	Zeta potential	Parameter to measure electrophoretic mobility which is the surface charge velocity of colloidal and nanosized materials distributed in a liquid under the influence of electric field	[8]
	Contact angle	Angle formed by the intersection of the liquid-solid interface and the liquid-vapor interface (geometrically acquired by applying a tangent line from the contact point along with the liquid-vapor interface in the droplet profile)	[9]
	Temperature tolerance	Basic feasibility of successful operation at the high temperature	[10]
Chemical performance	Chemical stability	Ability to withstand change from chemical contact	[11]
	Antifouling property	Ability of preventing the accumulation of fouling organisms	[12]
	Corrosion resistance	Ability of a material to withstand deteriorization of its surface or properties when exposed to its environment	[13]

The criteria for the membranes in microfiltration, ultrafiltration, nanofiltration, reverse osmosis, forward osmosis processes are compared in Table 2 by comparing pore size, rejected substances, and values.

Ceramic membranes have been hailed for their advantageous properties when compared to polymeric membranes. The advantages of ceramic membranes compared to polymeric membranes are often stated to be: (i) a relatively narrow pore size distribution and higher porosity, resulting in better separation characteristics and a higher flux, (ii) higher hydrophilicity resulting in high fluxes at low pressures, (iii) flux through ceramic membranes are more easily recovered after fouling, and (iv) higher mechanical stability and higher chemical stability resulting in longer membrane lifetimes even under extreme fouling and cleaning conditions [30–36]. With the enhanced properties, ceramic materials are well suited for challenging water purification processes, such as industrial wastewater, oil/water separations, and hazardous waste treatment. α-Al$_2$O$_3$ was proposed to be initially used as the raw material for the preparation of ceramic membranes [37]. Afterward, γ-Al$_2$O$_3$, zirconia, titania, and silica were reported as promising material used for membrane synthesis [38]. Recently several natural minerals and industrial wastes, which are in

abundance and need lower firing temperature than metal oxide materials, such as kaolin, bauxite, diatomite, dredge sediment, etc., emphasize the remarkable cost reduction of starting materials. These new generations of low-cost ceramic membranes have been broadly explored for separation and catalysis domains, such as treatment of colored wastewater, oil-water separation, produced water as well as recovery of the valuable component by concentration feed solution (acid, fruit juices, sugar and alcohols, etc).

2. Raw materials

The employment of minerals and waste in ceramic membranes manufacturing instead of the more expensive ceramic materials realized the significant reduction in cost, further adding great economic value to raw minerals that are widely available all over the world.

2.1. Mineral-based ceramic membrane

2.1.1. Clay

The ceramic membrane generally possesses an asymmetric structure composed of robust support and an active

Table 2
Criteria for the membranes in various applications

Process	Pore type	Pore size	Rejected substances	Application
Microfiltration	Macropores	>50 nm [14]	Yeasts; fungi; bacteria; oil emulsion	Domestic wastewater treatment [16]; oil-contaminated water treatment [17]; juice clarification [18]
Ultrafiltration	Macropores	2~50 nm [14]	Colloidal solids; viruses; proteins; polysaccharides; humics; nucleic acids	Oil-contaminated water treatment [19]; heavy metal removal [20]; textile wastewaters treatment [21]
Nanofiltration	Macropores	<2 nm [14]	Common antibiotics	Separation of electrolytes [22]; ions remove [23]; treatment of pesticide wastewater [24]
Reverse osmosis	Macropores	0.3–0.6 nm [15]	Organic antibiotics	Separation of electrolytes [22]; seawater desalination [25]; recycling process [26]
Forward osmosis	Macropores	0.3–0.6 nm [15]	Inorganic antibiotics	Pretreatment of seawater [27]; wastewater reclamation [28]; food processing [29]

layer with separation property, the formation mechanism of which was schematically elucidated in Fig. 1 [39]. The support with large pores, which provides mechanical strength as well as facilitates fluid transport, can be shaped by extrusion or isostatic pressing techniques [40,41]. The active layer with small pores plays a vital role in separation was generally prepared by slip-casting [42], dip-coating [43], and spin-spraying [44], and the cross-flow filtration [45]. The ceramic membrane support has been broadly explored for pretreatment in the wastewater treatment, whereas the support with an active layer was usually considered as a versatile microfiltration and ultrafiltration technique. Notably, the intermediate layer sometimes was fabricated between the support and the active layer as a function of pore size transition.

Clay minerals of SiO_2–Al_2O_3 system have been gaining recognition due to structural adsorption, rheological and thermal properties for a variety of applications [46]. The ratio of SiO_2 and Al_2O_3 varied with the clay kinds. Moroccan clay, which was essentially formed of 80 wt.% SiO_2 and 12.1 wt.% Al_2O_3, was used by Saffaj et al. [47] to prepare ceramic membranes support. The clay powder presented the diameter ranging from 1 to 40 μm, in which more than 80% was less than 5 μm. The porous tubular support was fabricated by firing Moroccan clay powders mixed with some organic additives after extrusion. The support showed an average pore diameter of 11 μm and a porosity of 43%. Zirconia was coated on the clay support to generate the microfiltration layer with average pore diameters of 0.23 μm and thickness of 10 μm. The ultrafiltration layer was constructed by the mixture of TiO_2–$ZnAl_2O_4$ on the microfiltration layer through the sol–gel routes. The thickness of the ultrafiltration layer is about 0.7 μm and the pore diameter is centered at 5 nm. This ultrafiltration membrane exhibited excellent separation properties in salts, heavy metal, and dye solutions.

Jana et al. [48] have employed the clay of IIT Guwahati which was mainly composed of 71.595 wt.% SiO_2 and 17.097 wt.% Al_2O_3 with wide diameter range to prepare two low-cost ceramic microfiltration membranes. Membrane A was fabricated only from clay, while small amounts of additives, such as sodium carbonate, sodium metasilicate and boric acid were added in membrane B. The average pore
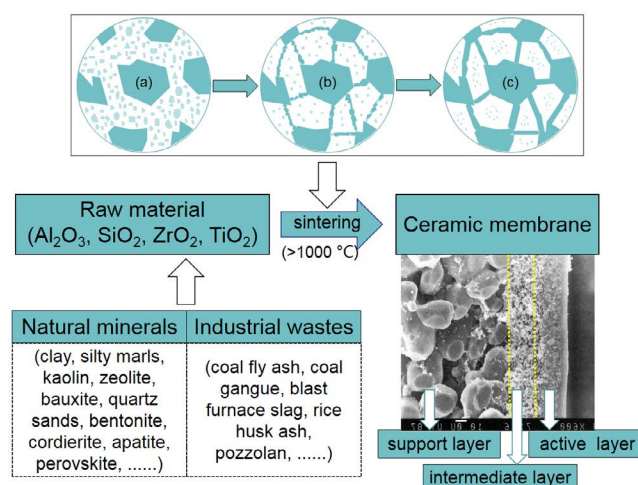

Fig. 1. Formation mechanism of ceramic membrane.

size, porosity, pore density and flexural strength of membrane B sintered at 1,000°C were 4.58 μm, 38%, 2.06×10^{10} m^{-2} and 11.55 MPa, respectively, which were much better than membrane A. The removal of chromate from aqueous solutions was executed by membrane B. A 100% rejection of chromate ions at a surfactant/chromate ratio of 1.0 was obtained, revealing good promise for the prepared low-cost membrane in heavy metals removal. The membrane cost was estimated to be \$19 m^{-2}, which was dramatically cheaper than the membrane prepared from the ceramic materials.

The clay of IIT Guwahati (70 wt.%) was also investigated to fabricate ceramic supports with kaolin (18 wt.%) and organic additives (12 wt.%), the average pore size and porosity of which were 1,093 nm and 37%, respectively [49]. The ultrafiltration layer was elaborated by dipping chitosan on the support, the average pore sizes of which were found to be within 760–13 nm. The ultrafiltration ceramic membrane with a pore size of 13 nm was selected for the removal of mercury and arsenic from an aqueous medium. Almost 100% removals were observed for both 500 μg L^{-1} mercury and 1,000 μg L^{-1} arsenic.

2.1.2. Silty marls

Silteous marls, as a kind of natural clay material, could also be chosen for ceramic membrane fabrication based on the lower firing temperature than metal oxide materials, excellent thermal stability, natural abundance, and low price.

Khemakhem et al. [50] have reported a two layers microfiltration ceramic membrane, the support of which was prepared to take the powder of silty marls as raw material. The support with pore diameters centered near 9.2 μm and porosity about 50% were obtained at the sintering temperature of 1,190°C. The silty marls were also introduced to deposit the microfiltration layer onto the supported by the slip-casting method. The mean pore size and water permeability of the membrane were identified to be 0.4 μm and 867 L h^{-1} m^{-2} bar^{-1} when the microfiltration layer calcinated at 1,000°C.

2.1.3. Kaolin

Kaolin is one of the widest clay materials, the price of which is at least about 100 times lower than that of alumina. The substantial energy conservation obtained by decreasing the sintering temperature from about 1,600°C to about 1,250°C and the relatively lower theoretical density of the prepared supports (2.8 g cm^{-3}) was the outstanding advantages when kaolin was applied in the ceramic membrane fabrication instead of alumina, enable kaolin a preferred raw material for porous ceramics [51].

Vasanth et al. [52] have addressed the development of ceramic microfiltration membranes from India kaolin, quartz, and calcium carbonate using the uniaxial dry compaction method. The prepared membranes sintered at 900°C presented the porosity of 30%, the flexural strength of 34 MPa, the average pore size of 1.30 μm, and identified as hydrophobic. The membrane was subjected to oil–water emulsion and bacteria separation experiments. Maximum rejection of 85% and 99% is obtained through the membrane for oil–water emulsion and *E. coli*, respectively.

Algerian kaolin DD2, mainly composed of 45 wt.% SiO$_2$ and 33.43 wt.% Al$_2$O$_3$ was selected by Medjemem et al. [53] for the elaboration of the membrane support. The diameter of the majority of support pores within 10 μm. Then, the Algerian kaolin DD3, which was mainly constituted by 43.69 wt.% SiO$_2$ and 37.53 wt.% Al$_2$O$_3$, was employed with CaO to fabricate intermediate layer. Finally, the zirconia top layer was deposited to form the separation layer, the average pore size of which was about 0.3 μm. This multilayer ceramic membrane showed a good permeability of 1,200 L h^{-1} m^{-2} for the water filtration and 100% microbial retention in the sterilizing solutions without heating.

The only stable crystalline phase in the kaolin mixture of SiO$_2$–Al$_2$O$_3$ system is mullite which has proven to strengthen the performance of the ceramic membrane. Various mineral materials can be used for the preparation of porous mullite ceramics, such as kyanite [54], bauxite [55], coal gangue [56], and kaolin [57] Guo et al. [57] prepared mullite ceramic membrane using natural mineral kyanite (53.41 wt.% Al$_2$O$_3$ and 39.74 wt.% SiO$_2$) as the raw material with Al(OH)$_3$ as a porogenic agent. From 1,450 to 1,500°C, the mullitization of kyanite generated needle-like mullite crystals, and the amount and size of needle-like mullite crystals increased with increasing temperature. When the sintering temperature above 1,500°C, however, the needle-like mullite crystals gradually developed into columnar in shape. The sintering temperature promoted the generation and development of mullite which formed skeleton structures and improved the apparent porosity and strength of the membrane. The micrographs variation of the kaolin-based ceramic membrane with sintering temperatures is displayed in Fig. 2. The mullite-based ceramic
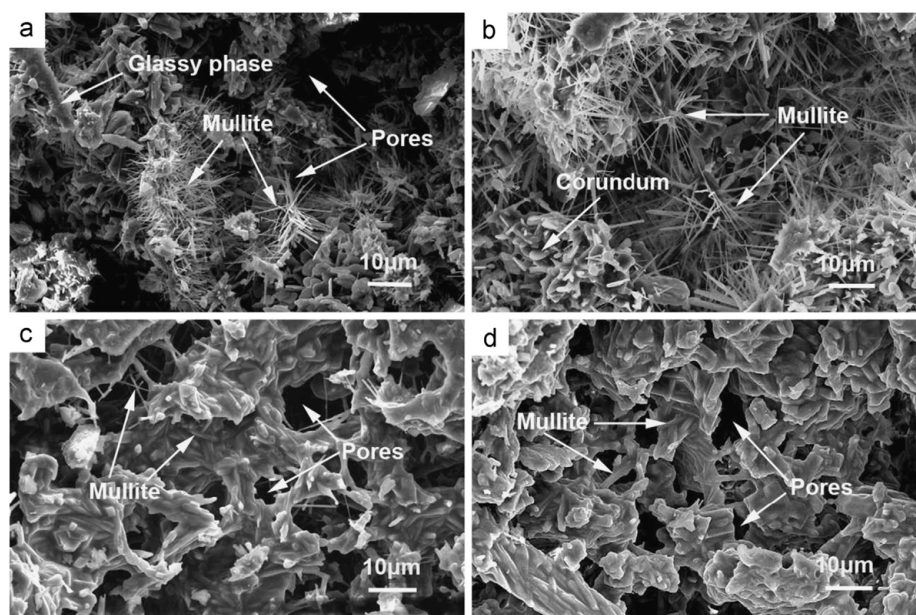

Fig. 2. Scanning electron microscopy (SEM) micrographs of kaolin-based ceramic membrane sintered at different temperatures, (a) 1,450°C, (b) 1,500°C, (c) 1,550°C, and (d) 1,600°C [21].

membrane prepared with 60 wt.% kyanite/40 wt.% Al(OH)$_3$ sintered at 1,500°C–1,550°C for 3 h exhibited an interlocked network microstructure composed of well development needle-like mullite crystals. High porosity (58.97%–60.71%), small average pore size (1.06–9.98 μm), excellent mechanical strength (7.72–9.63 MPa) and good nitrogen gas flux (4,952–5,322 m^3 m^{-2} h^{-1} at 0.4 MPa) were obtained.

Abbasi et al. [58] compared the mullite ceramic membrane prepared from kaolin, which was composed of 61.62 wt.% SiO$_2$ and 24 wt.%–25 wt.% Al$_2$O$_3$, with the mullite–alumina ceramic membrane prepared from kaolin and alumina powder. The oily wastewaters treatment results showed that the mullite ceramic membrane has the highest rejection of 93.8% which is much higher than the mullite–alumina ceramic membrane with 75% alumina (81.3%).

2.1.4. Zeolite

Zeolite minerals, known as natural sedimentary or naturally occurring zeolites, are mainly composed of aluminosilicates with a three-dimensional framework structure bearing AlO$_4$ and SiO$_4$ tetrahedra, as shown in Fig. 3 [59]. Natural zeolite mineral could be used as the raw material of mineral-based ceramic membrane because of its weak swelling capacity in water, simplicity for coating membrane on a porous support, as well as the specific sintering process due to its multiple compositions. The inter-particle active pores with separation function in membrane could form when the specimens are sintered.

Dong et al. [60] have explored the probability of taking natural heulandite zeolite mineral as raw material to fabricate the intermediate layer and active layer on the tubular porous zeolite ceramic support by a dip-coating process. The low sintering temperature (between 850°C and 950°C) caused low energy consumption because of the existence of impurities alkali metal oxides in the natural zeolite mineral as a fluxing agent. The intermediate layer with average pore size in the range of 0.69–1.10 μm and the active layer with average pore size 0.54 μm could be obtained Nitrogen gas permeation flux and pure water permeation flux of the resulting membrane was evaluated to be 1.96 × 10^5 and 3.20 × 10^3 L m^{-2} h^{-1} × 10^{-5} Pa^{-1} with the trans-membrane pressure of 0.1 MPa at room temperature, respectively, indicating these low-cost mineral-based membranes may be the potentially excellent candidates for use in the micro-filtration application.
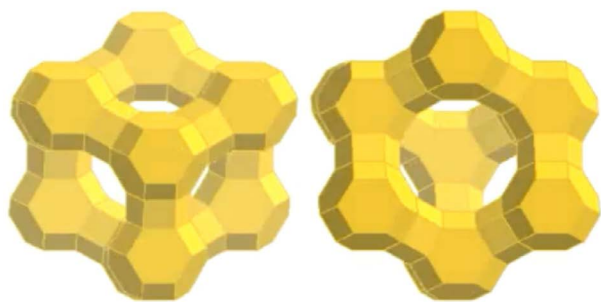

Fig. 3. Structure of zeolite.

2.1.5. Bauxite

Bauxite, a naturally occurring and abundant mineral predominantly consist of Al$_2$O$_3$, a small amount of SiO$_2$ and other metal oxides such as TiO$_2$ and Fe$_2$O$_3$ is suitable for replacing industrial-grade alumina to fabricate low-cost porous ceramic membranes without any industrial refinement [61].

Bauxite mineral incorporated with ZnO was introduced to elaborate a spinel-based ceramic membrane (ZnAl$_2$O$_4$) support which could reuse the natural mineral as well as stabilize zinc [55]. Five Zn-doped membranes were fabricated and defined as ZnAlx (where x stands for the Al/Zn molar ratio, x = 2, 2.5, 3, 4, and 8, respectively. Particularly, Al represents the sample prepared from only calcined bauxite without ZnO loading. The ZnAl$_2$O$_4$ spinel phase expansion from 1,000°C to 1,300°C together with the general densification due to amorphous liquid SiO$_2$ caused the highest porosity, as high as 44%, of ZnAl$_4$ membrane support among all the investigated compositions. Compared with the Al membrane, ZnAl$_4$ membrane support is reinforced by the ZnAl$_2$O$_4$ phase and inter-locked mullite crystals. Besides, an increase in average pore diameter and gas flux was also observed in ZnAl$_4$ membrane support. Moreover, zinc was proved to be stabilized successfully by the formation of ZnAl$_2$O$_4$ spinel structure through the prolonged leaching experiment, which is presented in Fig. 4.

2.1.6. Quartz sands

Natural quartz sands is a widely used raw material around the world, in which the majority of crystal silicon dioxide makes them attractive for the creation of ceramic membranes.

The fabrication of multi-layer ceramic membranes form the natural quartz raw material was studied by Şan et al. [62]. Porous tubular ceramic supports with the size of pores 50–100 mm, open porosity 26%–28% and strength on compression around 30 MPa were obtained on the basis of quartz raw materials from Mongolia. Microfiltration layers were applied on the outer surface of tubular supports using the suspension of quartz sand with the additives of crushed quartz. The average pore size of 5.3 mm, the air permeability coefficient of (4.17–4.41) × 10^{-13} m^2, water productivity of (46.3–48.0) L h^{-1} m^{-2} bar^{-1} and excellent mechanical strength, indicating this multi-layer ceramic membrane was perspective for wide use in microfiltration processes.

2.1.7. Bentonite

Bentonite, as a type of clay rock, has been used as adsorbents, catalysts and ion exchanger in many industrial fields due to its outstanding physical and chemical properties, that is, large specific surface area, cation exchange capacity, and adsorptive affinity for organic and inorganic ions [63,64]. The chemical components of bentonite are siliceous (SiO$_2$) and aluminous (Al$_2$O$_3$), enable this material to be the starting material of the ceramic membrane.

Bouazizi et al. [65] reported the development and characterization of a ceramic membrane prepared from natural bentonite extracted from the vicinity of Nador, Morocco. The membrane with a porosity of 32.12%, the mean pore
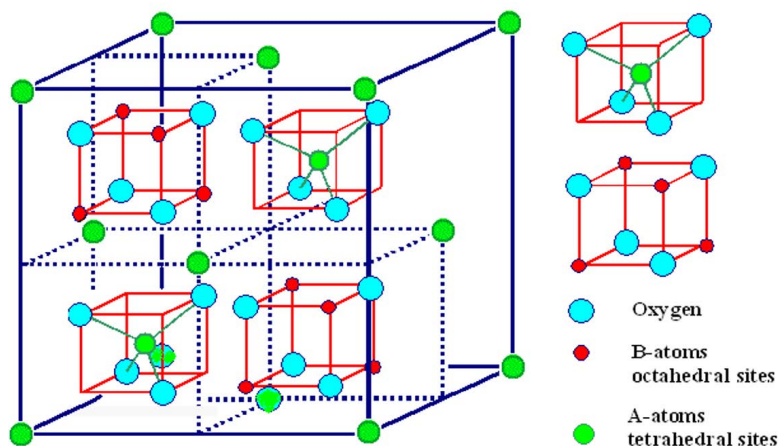
Fig. 4. Structure of AB_2O_4 spinel.

size of 1.70 μm, the flexural strength of 22 MPa and good chemical stability both in acidic and alkaline media were obtained at the optimal sintering temperature of 950°C. The water permeability of the elaborated membrane was 520 L h^{-1} m^{-2} bar^{-1} after 2 h of filtration. The removal percentage of suspended matter for the tannery and textile effluents was between 94% and 99%, leading to complete discoloration of textile wastewater.

2.1.8. Cordierite

The cordierite with the ideal chemical formula of $Al_3Mg_2AlSi_5O_{18}$ occupies a special place among these ceramics because of its remarkable thermal and chemical stability, thermo-mechanical resistance, as well as low thermal expansion properties and dielectric constant [66,67], which makes it suitable to be applied in harsh environments such as refractory products for industrial furnaces and electric heaters [68], heat exchangers for gas turbines, thermal shock resistant tableware, monolithic catalyst, supports for diesel cars, as well as membrane filters in some works [60,69].

Dong et al. [70] have prepared tubular ceramic membranes supports by extrusion followed by sintering using industrial-grade cordierite powders as the main starting materials to verify the practicability of this membrane in the strong corrosive environment. The fabricated cordierite ceramic membrane showed an average pore diameter of 8.66 μm, open porosity of 36.20%, nitrogen gas flux of 1.45×10^4 L m^{-2} h^{-1} and linear thermal expansion coefficient of 4.34×10^{-6}°C^{-1} at the optimized sintering temperature in the vicinity of 1,380°C. The chemical resistance tests were carried out in the sodium hydroxide and sulfuric acid solutions under the boiling condition, respectively. The cordierite supports which exhibited better thermal alkali resistance when compared with the as-used alumina supports were proved not suitable for the application of a strong acid environment due to the quick dissolution of Mg and Al elements and the subsequent generation of free amorphous silica. Low cost of starting materials, low sintering temperature and good alkali resistance enable this cordierite-based ceramic membrane great economic significance and applied value.

2.1.9. Apatite

Apatites with the general formula of $A_5(BO_4)_3Y$ are very abundant in the phosphate mines and biological environment, in which M presents Ca, Sr, Ba, Pb, etc.; X presents P, As, Si, etc.; Y presents various anions, such as OH–, F–, Cl– or other groups [71,72]. In general, structure drawings highlight only the relatively regular BO_4 tetrahedra, while other features are usually grouped as "irregular" polyhedra, in which the apatite prototype $Ca_5(PO_4)_3F$ structure is exhibited in Fig. 5. The wide range of physicochemical properties, the property of trapping heavy or radioactive metals effectively, and the similarity to biomaterials enabled them as a raw material in many applications like artificial fertilizers, catalysts, osseous prostheses, etc., indicating the apatite is appropriate material for the development of microfiltration membranes applied to the industrial wastewater treatment.

Masmoudi et al. [73] have prepared the tubular ceramic membrane support with a highly uniform porous structure by natural apatite. The active layers were deposited on the tubular support by the "slip-casting" process from lacunary hydroxyapatite synthesized (HA) and from natural apatite (AB) to prepare membrane MS and membrane MB, respectively. The average pore diameters and porous volume of the active layer are respectively about 0.25 μm and 47% for MS and 0.2 μm and 45% for MB. The obtained membranes were tested to treat cuttlefish effluents. A very significant decrease of turbidity (>99%), chemical oxygen demand (COD 82%), the number of total germs (100%), and conductivity (74%) was obtained.

2.1.10. Perovskite

Perovskites described by the general formula ABO_3 where the cation A is surrounded by twelve equidistant oxygen atoms and the cation B is surrounded by six oxygen atoms, the structure of which is shown in Fig. 6 [74]. Perovskite oxides where the A and B-sites were partially occupied by elements from the rare earth, alkali or alkaline families such as La, Na, Ca, Sr or Ba could create oxygen vacancies and thus allows for oxygen ion conduction [75,76].
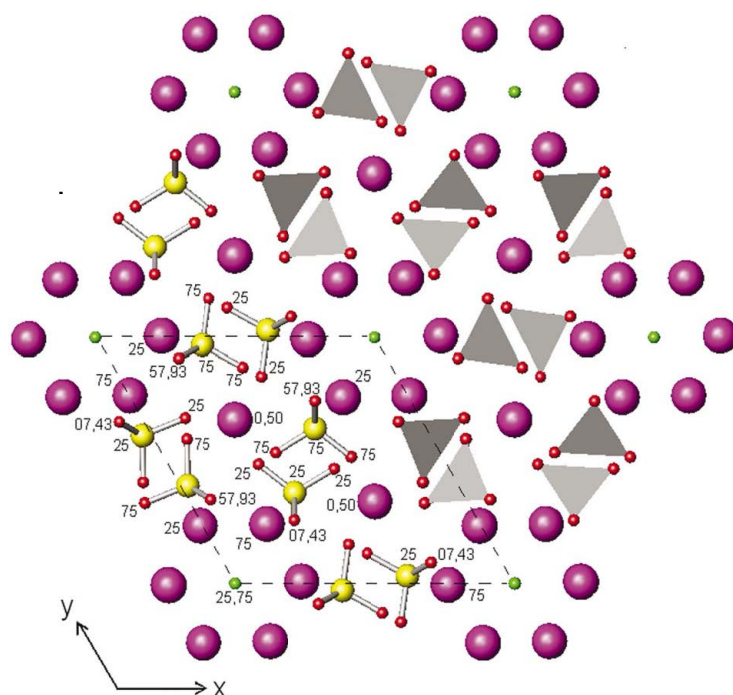
Fig. 5. The [109] projection of fluorapatite $Ca_5(PO_4)_3F$ represented in the conventional way with PO_4 units highlighted, like a ball and stick or tetrahedral representations, and with the oxygen coordination to the Ca cations de-emphasized.
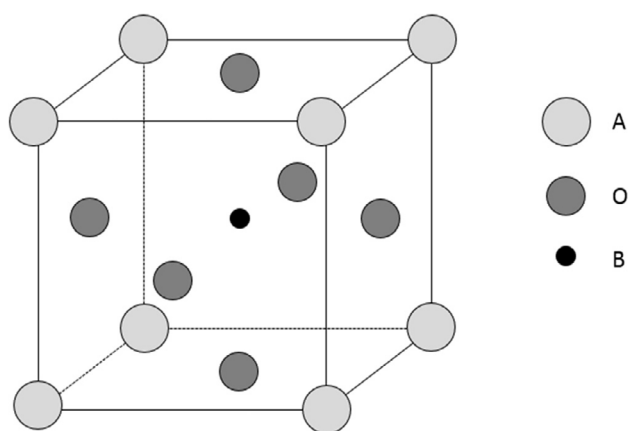

Fig. 6. Structure of ABO_3 perovskites.

When doped with different cations, zirconium-doped perovskite-type membrane materials of $BaCo_{0.4}Fe_{0.6-x}Zr_xO_{3-\delta}$ (x = 0–0.4) with mixed oxygen ion and electron conductivity were synthesized through a method of combining citric and ethylenediaminetetraacetic acid (EDTA) acid complexes [77]. It was showed that the incorporation of the proper amount of zirconium into $BaCo_{0.4}Fe_{0.6}O_{3-\delta}$ could stabilize the ideal and cubic structure of perovskite. Studies on the oxygen permeability of the as-synthesized membrane under air/He gradient indicated that the content of zirconium in these materials had great effects on oxygen permeation flux, the activation energy for oxygen permeation and operation stability. The high oxygen permeation flux of 0.90 mL cm^{-2} min^{-1} at 950°C, the single activation

energy for oxygen permeation in the range of 600°C–950°C and the long-term operation stability at a relatively lower operating temperature of 800°C were achieved for the $BaCo_{0.4}Fe_{0.4}Zr_{0.2}O_{3-\delta}$ material.

Chen et al. [78] have prepared zincum-doped ceramic membrane materials based on $BaCo_{0.4}Fe_{0.4}Zn_{0.2}O_{3-\delta}$ with $0 \leq x \leq 0.2$ via the same method. The zincum-doped ceramic membrane exhibits excellent structure stability and reversibility. The introduction of small amounts of Zn on the B-site and the doping of barium on the A-site could diminish the reduction of cobalt and iron, which stabilizes the structure. An oxygen permeation flux of 0.65 mL min^{-1} cm^{-2} was obtained at 950°C and the membrane was steadily operated for more than 100 h in the oxygen permeation.

2.1.11. Pozzolan

The natural pozzolan, which is a cheaper and environment-friendly raw material, has been largely preserved in Morocco. The chemical composition (especially rich in MgO and SiO_2, Al_2O_3), good chemical and mechanical resistance enable pozzolan as the starting material of the ceramic membrane.

Achiou et al. [79] described the manufacturing of asymmetric pozzolan-based ceramic microfiltration membrane composed of tubular support and an active layer. The support was prepared by sintering pozzolan powder, clay, and some organic additives at a low temperature of 950°C and showed a porosity of 41.2%, an average pore diameter of 8.18 μm and permeability of 2,120.3 L m^{-2} h^{-1} bar^{-1}. The active layer was prepared by crossflow filtration of suspension containing the pozzolan powder, polyvinyl alcohol and water followed by sintering at 950°C. The defect-free

active layer with 1.12 µm in pore size diameter, 5.52 µm in thickness and 1,444.7 L m^{-2} h^{-1} bar^{-1} in permeability exhibited a good performance regarding seawater pretreatment for desalination. A high turbidity rejection of 98.25% as well as a good COD retention of 70.77% were achieved.

2.2. Waste-based ceramic membrane

2.2.1. Coal fly ash

Waste fly ash, classified as one of the hazardous industrial solid wastes, is a by-product of coal incineration in thermal power plants and produces serious environmental pollution. One of the effective ways for recycling fly ash in significant quantities is to take it as a substitute for cement in construction and other civil engineering applications [80,81]. During the last years, considerable research efforts have been devoted to the integration of fly ash in the manufacture of silicate-based materials, that is, bricks, tiles, conventional porous ceramic products [82,83]. Recently, the substitution of industrial-grade alumina by a SiO_2–Al_2O_3–MeO system coal fly ash, in which Me represents metal elements like Na, K, Ca, Mg, Fe, etc., for ceramic membrane preparation, has already been realized [84].

Fang et al. [85] have developed two layers of fly-ash-based ceramic membrane and evaluated the permeability and anti-fouling property of this membrane for microfiltration of particle suspension and oil-in-water emulsion. The asymmetric membrane was elaborated by slip-casting refined fly ash onto the inner surface of macroporous fly-ash-based tube support. After continuously running for 10 h without backwashing, a permeate flux of approximately 2,530 L m^{-2} h^{-1} and a particle rejection efficiency of 99.9% can be maintained during microfiltration of particle suspension under optimum operating conditions. A permeation flux of 159 L m^{-2} h^{-1} and an oil rejection efficiency in excess of 95% was obtained in microfiltration of oil-in-water emulsion under optimum operating conditions. This fly-ash-based membrane exhibited lower membrane fouling resistances and thus a higher competition comparing to the other available inorganic membranes in both filtration processes.

The fly ash was also investigated to elaborate on a ceramic microfiltration membrane composed of macroporous support and an active layer by Jedidi et al. [80] for application in the clarification and the decoloration of the effluents coming from the dying industry. The macroporous support obtained from heating the original mineral coal rock without prior grinding at 800°C and showed an average pore diameter and porosity of about 4.5 µm and 51%, respectively. The active layer obtained from depositing the finely ground mineral coal powder onto the support with subsequent sintering at 800°C. The active layer was characterized as defect-free, the thickness, mean pore diameter, and water permeability were determined to be 20 µm, 0.25 µm, and 475 L h^{-1} m^{-2} bar^{-1}, respectively. The application of this fly-ash-based membrane to the treatment of the dying effluents generated by the washing baths in the textile industry showed a stable permeate flux of around 100 L h^{-1} m^{-2}, COD removal of about 75%, a total color removal, and very low permeate turbidity of 0.5 NTU, respectively. The comparative performances in terms of permeate flux and efficiency with a commercial alumina microfiltration membrane indicated this coal fly ash as an appropriate material for the application in the industrial textile wastewater treatment.

2.2.2. Coal gangue

Another industrial solid waste coal gangue, which is one of the by-products during coal mining, caused serious atmospheric pollution from combustion and water pollution from leaching of heavy metal ions [86,87]. Many approaches emphasized recycling of coal gangue via traditional construction materials, such as cement [88] and brick [89]. In general, the main chemical composition of coal gangue is SiO_2, Al_2O_3, Fe_2O_3 and some other minor oxide such as K_2O and TiO_2, making it to be a potential source in the fabrication of ceramic membrane [90]. Notably, the content of SiO_2 in coal gangue is generally as high as 70% compared with other industrial wastes and minerals.

Lü et al. [57] have fabricated porous ceramic membrane supports from coal gangue and bauxite. The as-fabricated supports presented a porous microstructure of sintered aluminosilicate glassy particles embedded with gradually grown mullite crystals from 1,200 to 1,500°C. The maximum nitrogen gas flux of 5.84×10^3 L m^{-2} h^{-1} was achieved at 1,400°C.

2.2.3. Blast furnace slag

The blast furnace slag, which is a by-product of the steel industry, was also employed as the main starting material to fabricate the free sintering and self-supported ceramic membranes [91]. The SFS was firstly alkali-activated and then poured into the stainless steel mold which was pressed by hydraulic pressing machine. All stages of synthesis and testing are conducted at 24°C ± 1°C. The optimum conditions of the most effective parameters such as drying time, hydraulic pressing pressure, and pressing time were determined by Taguchi's L$_9$ orthogonal array. Two optimal membranes for COD removal and permeation flux were identified through performing cross-flow filtration of gas oil in water emulsion. The COD optimal membrane with an average pore diameter of 0.07 µm and a maximum pore diameter of 0.29 µm was obtained at a hydraulic pressing pressure of 400 bar, drying time of 6 h and pressing time of 5 min. This ultrafiltration (UF) membrane exhibited 100% COD removal and pure water permeation flux of 106 kg m^{-2} h^{-1}. The permeation flux optimal membrane with a mean pore diameter of 0.66 µm and a maximum pore diameter of 2.43 µm was obtained at a hydraulic pressing pressure of 225 bar, drying time of 8 h and pressing time of 30 min. The pure water permeation flux of this microfiltration (MF) membrane reached 1,960 kg m^{-2} h^{-1}.

2.2.4. Rice husk ash

Hubadillah et al. [92] reported a green ceramic hollow fiber membrane, derived from rice husk ash (RHA) using the combined phase inversion and sintering technique at lower sintering temperature of 1,200°C, comparing to conventional alumina material (1,500°C). The RHA suspension was prepared and extruded from the stainless steel syringes

at a constant flow rate. The phase inversion occurred when the precursor hollow fibers were immersed in water. After drying, the hollow fibers were sintered to get an asymmetric membrane structure with finger-like and sponge-like features, as presented in Fig. 7. The membrane presented the average pore size of 1.2 μm, the porosity of 36.7%, the excellent mechanical strength of approximately 58.83 MPa, and a high flux of 301.3 L m^{-2} h^{-1}, respectively. It effectively acts as both separator and adsorbent of heavy metals in a single-step process with high separation efficiency up to 99% removal of zinc [Zn(II)], lead [Pb(II)] and nickel [Ni(II)], proving this RHA-based ceramic membrane is an attractive, effective and environmentally friendly material in water treatment.

3. Ceramic membrane application

3.1. Liquid treatment

3.1.1. Solid removal

Several conventional technologies, including the chemical precipitation, chemical/electrochemical reduction, solvent extraction, and electrolysis of charged water [93], have been successfully used for the removal of solid matter from wastewater. However, these techniques suffered from technical limitations, economic viability, low removal efficiencies, as well as secondary contamination. The inorganic membranes process, particularly the ceramic membranes, becoming an efficient alternative for solid removal by their intrinsic properties notably in terms of thermal and chemical stability and high mechanical strength.

Zhou et al. [94] reported a new ceramic microfiltration membrane, which composed of α-alumina tubular supports and attapulgite nanofibers separation layer, for solid separation. The defects-free microfiltration membrane showed an average pore size of 0.250 μm, a thickness of approximately 6.7 μm, and a pure water flux of 1,540 L m^{-2} h^{-1} bar^{-1}. The separation performance was tested via a rejection experiment using calcium carbonate granules with an average particle diameter of 1.0 μm and a concentration of 1.0 g L^{-1} at 20°C. A 100% rejection of the calcium carbonate particles in suspension, and showed a steady permeate flux of approximately 980 L m^{-2} h^{-1} bar^{-1} were observed. In addition, the membrane can be easily regenerated by backwashing without any damage.

Belibi et al. [95] reported the porous ceramic membrane support which elaborated from natural and local Cameroonian clay (Wak village) and evidenced the excellent separation characteristic of clay powder. The support, which was prepared by firing at 1,100°C for 2 h under air after shaping and pressing the mixed raw material, showed adequate porosity of 42% and thus could be used as a microfiltration filtering membrane. The solid separation characteristic of the elaborated membrane as evidenced by performing filtrations of aqueous suspensions of clay powder at concentrations of 2 and 1 g L^{-1} as a function of cycle times. The intrinsic rejections were found to decrease with an additional cycle. The maximum retention rate was 97% after cycle 4.

3.1.2. Dye removal

As the long-term water pollutants, most of the dyes used in the textile industries were stable to ultraviolet light and resistant to biodegradation. Although effective, the conventional methods were still limited to economic feasibility,
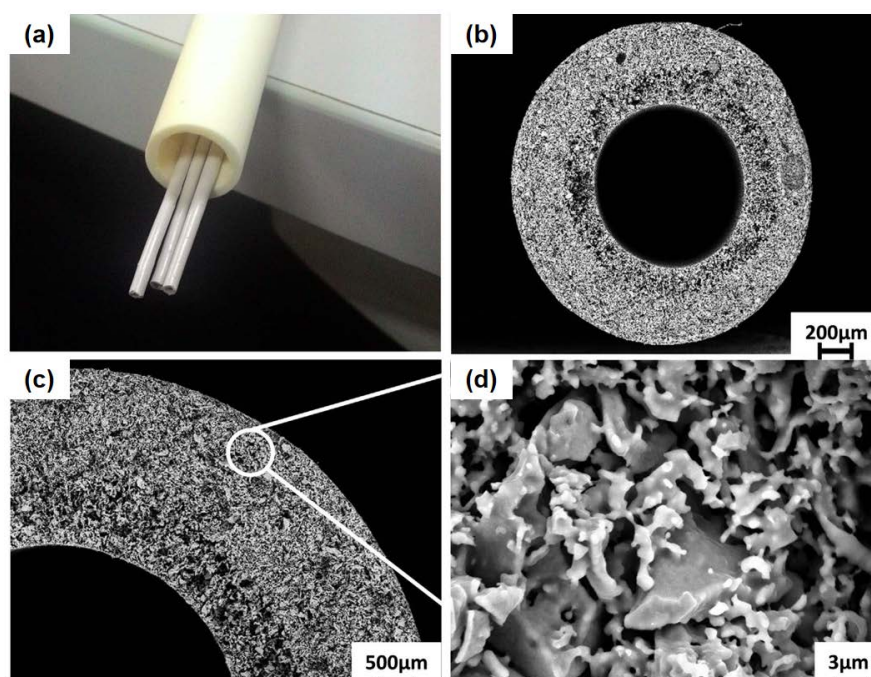

Fig. 7. SEM images of an asymmetric membrane structure with finger-like and sponge-like features (a) digital image, (b) overall cross-sectional SEM image, (c) local enlarged cross-sectional SEM image, and (d) SEM image at high magnification.

technical difficulties, and separation efficiency. The need for high-quality effluent made an increasing incentive to develop a more effective option for dye removal. Over the last years, extensive applications of ceramic membrane separation processes made it highly efficient and especially beneficial in dye removal.

Bouazizi et al. [65] reported the elaboration of two layers of flat ceramic membranes and elucidated its separation efficiency in dye wastewater filtration. The membrane support, which was successfully fabricated from 70% of natural bentonite and 30% of micronized phosphate, was satisfying in terms of porosity (34.06%), average pore size (1.8 μm), water permeability (725 L m^{-2} h^{-1} bar^{-1}) and good mechanical strength (14.6 MPa). The defects-free TiO$_2$ active layer was deposited on the resulting support by spin-coating to present the pore diameter of approximately 72 nm and water permeability of 33 L m^{-2} h^{-1} bar^{-1} respectively. The Direct Red 80 solution was employed to test the separation efficiency of the UF membrane for dye wastewaters. A high dye rejection of 98 ± 2% at the feed concentration of 100 ppm is observed.

Cheng et al. [96] developed a positively charged microporous ceramic membrane which was proved to be a potential strategy in the field of dye removal based on the electrostatic adsorption principle. The internal surface of the highly porous ceramic membrane was coated with a uniformly distributed electropositive nano-Y$_2$O$_3$ coating. The pressurized filtration tests were introduced to evaluate the dye removal performance using Titan Yellow aqueous solution. A flow rate of 421 L m^{-2} h^{-1} under the trans-membrane pressure of 0.03 bar and effective removal efficiency of Titan Yellow with feed concentration of 10 mg L^{-1} between pH 3 to 8 were elucidated. With the enhancement of the surface charge property, the removal rate increased to its maximum of 99.6%, convincing that there will be a broad market for the application of charged ceramic membranes in the field of dye removal.

3.1.3. Ion removal

Most types of ceramic membranes separate the particles larger than the pore size of the membrane by sieve effect. However, Wei et al. [97] have developed a two-layer ceramic membrane that presented a large water flux under low-pressure values, and separated phosphate ions much smaller than the pore size. The ceramic support was prepared using 80 wt.% clay and 20 wt.% fly ash and had the appropriate porosity of 36.2% and compressive strength of 17.9 MPa. The attapulgite layer was sintered on the support to obtain the pore size distribution between 5 and 53 nm. The excellent pure water flux of 52.89 L m^{-2} h^{-1} under 0.3 MPa and a high phosphate rejection efficiency of nearly 90% when the pH value was between 9.5 and 10.5 were revealed.

3.1.4. Heavy metal removal

Wastewater with a large number of heavy metal ions originated from different fields like metal plating, coal mining or metal mining, which were proposed to be one of the serious environmental problems worldwide. The intensive investigations so far have been devoted to the removal of these ions since these pollutants were not only non-biodegradable but toxic even at low concentrations. Metals like mercury and arsenic found in industrial effluents and groundwater posed serious threats to the environment. The general methodologies for removal of mercury ions (safe limit 2 ppb) from aqueous solution were absorption [98], chelation-enhanced method [99] and electrocoagulation [100]. Arsenic (safe limit 10 ppb) could be separated by inorganic and organic adsorbents [101] including bioadsorbents [102]. However, these methods suffered from incomplete metal removal and secondary contamination [103]. With the progress of technology, membrane processes like reverse osmosis have been applied for the removal of heavy metal ions.

The low-cost ceramic membrane, composed of clay support and a chitosan layer, showed the pore size of 13 nm and be used for the removal of mercury and arsenic from wastewater [496]. It was found that though the metal concentration in the permeate increased with time, initially 100% removal was observed at the concentration of 500 μg L^{-1} for both the metals. A comparative experiment of the heavy metal removal efficiency among reverse osmosis, nanofiltration and this ceramic membrane process revealed a 100% removal in the present ceramic membrane process at very low pressure, indicating this low-cost ceramic membrane may play a superior role over reverse osmosis and nanofiltration process in the heavy metal removal.

Kaolin-based ceramic membrane support with an average pore diameter of 1.32 μm, the porosity of 30% and flexural strength of 34 MPa was elaborated by Vasanth et al. [104] and explicated the removal efficiency of heavy metal ions. The removal of Cr(VI) was found to increase at lower pH, higher biomass concentration and lower metal ion concentration. The maximum removal of Cr(VI) was found to be 94% with the permeate flux of 2.07 × 10^{-5} L m^{-2} s^{-1} at the pH of 1 and the metal ion concentration of 100 mg L^{-1}.

3.1.5. Oily wastewater treatment

Oil in wastewaters could be classified into floated oil, dispersed oil (about 90 wt.%), emulsified oil (about 10 wt.%), and dissolved oil (<0.5 wt.%) [105,106]. Floated oil and dispersed oil have relatively large droplet size (>10 μm) so that can be mechanically removed. Emulsified oil (<10 μm), which is usually referred to as an oil in water (O/W) emulsion, is intensively produced daily by industries such as crude oil production, oil refining, transportation, cosmetics, textile, etc [107,108]. O/W emulsion is difficult to be removed since the tiny oil droplets are stabilized by surfactants which considerably reduce the interfacial tension between oil and water [109]. Conventional treatment techniques, including dissolved air flotation, gravity separation, coalescence separation, etc., are not efficient to remove tiny oil droplets and thus difficult to meet the more and more stringent standards for discharge [110,111]. Membrane separation is one of the promising alternatives since they are high efficiency, thermal and chemical stability, excellent pressure resistance, long lifetime, do not require chemical additives, catalytic property and more economical compared to conventional separation techniques [112,113].

Mittal et al. [114] prepared a low-cost hydrophilic ceramic membrane with clay-kaolin support and a cellulose acetate layer and clarify its separation property in O/W emulsion treatment. The high rejection was found to be obtained at high oil concentration and long running time. The maximum rejection of 93% with a permeate oil concentration of 14 mg L^{-1} was observed at 41 min.

3.1.6. Juice clarification

Amongst several beverage processing sectors, citrus fruits constituting orange, lemon, pineapple and mosambi are prominent due to their wider availability, low cost as well as high nutrition value to human health. Citrus fruits primarily constitute both lower molecular weight compounds (such as sugar, acid, salt, flavor, aroma compounds, etc.) as well as higher molecular weight polysaccharides (such as pectic material cellulose, hemicellulose, etc.) in addition to haze causing proteins and microorganisms. The presence of pectic material and protein in fruit juice is responsible for cloudiness and post-bottling haze formation as well as their fermentation during long storage [115]. Recently, considerable research have focused on the ultrafiltration and microfiltration of mosambi [116], orange [117], lemon [118], grape [119], apple [120], carrot [121], watermelon [122], blood orange [123] and pineapple juice. The objective of clarification of fruit juice using membrane filtration is to eliminate the high molecular weight pectic material and its derivatives and retain low molecular weight solutes.

Nandi et al. [124] reported a kaolin-based microfiltration ceramic membrane support and its application for both centrifuged mosambi juice (CJ) and enzyme-treated centrifuged mosambi juice (ETCJ) treatments. The average pore diameter, total porosity and hydraulic resistance of the membrane were evaluated as 0.285 μm, 23.6% and 9.26×10^{11} m^2 m^{-3}, respectively. The dead-end MF experiments declared that the total soluble solids, pH, acidity and density of both CJ and ETCJ were not varied significantly. However, significant improvement in juice color, clarity and alcohol insoluble solid was observed. The clarified juice can be stored in refrigerated condition for more than 30 d without significant change in juice quality, inferring this low-cost ceramic membrane support was promising for mosambi juice processing.

3.1.7. Seawater desalination

Production of drinking water by seawater desalination becomes more and more a worldwide preoccupation, especially in countries that suffer from few rainfalls like Morocco. The pretreatment is essential in the seawater desalination to prevent or minimize the bioencrassage, scaling and clogging of the reverse osmosis membranes [125,126]. The classical methods (i.e. the coagulation and flocculation processes) for seawater desalination pretreatment generate a huge amount of sludge that must be eliminated later [127]. Microfiltration membranes particularly the ceramic membranes can be an efficient alternative to the conventionally used various types of methods.

Achiou et al. [79] described the pozzolan-based tubular ceramic membrane with the average pore size and water permeability parameters of 0.36 μm and 1,444.7 L m^{-2} h^{-1} bar^{-1} respectively for seawater desalination pretreatment. The filtration of raw seawater showed a high turbidity rejection of 98.25% as well as a good COD retention of 70.77%, indicating excellent pretreatment property.

3.1.8. Sterilization

Membrane filtration is a viable option for removing contaminants, including oil, dye, toxic heavy metal ions, salts, etc., from aqueous solutions. Recently, membrane technology is becoming very important to sterilize the solutions media in various industrial fields, such as food, medical industries and biology, aiming at reducing the risks of contamination [128]. Compared to the conventional sterilization by thermal, radiation or chemical methods leaves killed microbial cells in the solution, membrane microfiltration removes these species [129,130]. Besides, the membrane technique is particularly suited to the separation and purification of thermally sensitive liquids since it operates at relatively low temperatures and involves no phase changes or chemical additives.

A multilayer ceramic membranes, which was composed by the support of kaolin, an intermediate layer of anorthite, and the top layer of zirconia, was successfully fabricated and used for the sterilization and preservation of thermolabile substance of plants medium culture [53]. No evidence of microbial growth was observed in the filtrate sample, demonstrating that the ceramic membrane had completely eliminated microflora from the medium culture. Furthermore, this filtration allowed preserving the quality of organic thermolabile substances. The membrane sterilization method was proved to be simple, inexpensive, non-destructive and a good way of quickly sterilizing solutions without heating.

The low-cost kaolin based ceramic membrane generated from Vasanth et al. [104] with a porosity of 30%, the flexural strength of 34 MPa, the average pore size of 1.30 μm was also inferred for the retention of bacteria. The bacteria rejection was revealed to increase with the feed concentration. The maximum rejection of 99% at the feed concentration of 6×10^5 CFU mL^{-1} was observed.

3.2. Gas separation

3.2.1. Oxygen permeation

Another practical application of the ceramic membrane are oxygen separation, where the dense oxygen selective membrane should possess excellent stability under strongly reducing atmosphere at elevated temperatures (>700°C), high oxygen permeability under operation conditions, good mechanical strength for constructing the membrane reactor or permeator, and cheap for large-scale industrial applications.

Zincum-doped perovskite-type ceramic membrane could be synthesized using combining citric acid and EDTA complexing method and reported to selectively separate oxygen from the air at elevated temperatures [78]. The membrane-based on BaCo$_{0.4}$Fe$_{0.4}$Zn$_x$Zr$_{(0.2-x)}$O$_{3-\delta}$ ($0 \leq x \leq 0.2$) displayed an oxygen permeation flux of 0.65 mL min^{-1} cm^{-2} at

950°C and single activation energy of 67 kJ mol^{-1} for the oxygen permeation in the temperature range of 600°C–950°C. The membrane-based on $BaCo_{0.4}Fe_{0.6-x}Zr_xO_{3-\delta}$ ($x = 0$–0.4) illustrated the high oxygen permeation flux of 0.90 mL min^{-1} cm^{-2} at 950°C, the single activation energy for oxygen permeation in the range of 600°C–950°C [77]. Accompanied by oxygen permeability, the long-term operation stability, structural stability, and reversible stability were also achieved for the above perovskite-type ceramic membranes, manifesting that these membranes were promising for use in the pure oxygen required industrial processes.

3.2.2. CO₂ adsorption and separation

The increased concentration of greenhouse gases like carbon dioxide in the atmosphere has been one of the most urgent global environmental concerns due to its climate-changing potential, and accordingly, the development of strategies towards mitigation of CO_2 and other greenhouse gases is of great importance. In previous studies, preliminary investigations on CO_2 transfer by physicochemical absorbents, oceanic or geological sequestration were carried out [131]. While some recent approaches focus on membrane driven separation processes since the specific zeolitic imidazolate frameworks (ZIF) ceramic membranes, where Si–O–Al bridges in zeolites are replaced by M-Im-M (M = Zn, Co, In, Cu; Im = imidazolate), possess exceptional thermal and chemical stabilities, large internal surface areas, coupled with uniform but tunable cavities. For easy visualization, the framework of ZIF-8 is described in Fig. 8.

It has reported that a Si_3N_4 hollow fiber supported ZIF membrane was synthesized by a one-step hydrothermal method and could be potentially used in CO_2 selective adsorption and separation [132]. The CO_2 initially adsorbed in the edge of the breather hole and then blocked the micropores partially. The strong CO_2 adsorption in the ZIF membrane together with the interactions of adsorbed CO_2 molecules with CO_2 passing through caused the decrease of CO_2 permeance from 2.84×10^{-7} mol m^{-2} Pa^{-1} s^{-1} to 1.15×10^{-7} mol m^{-2} Pa^{-1} s^{-1} in the first hour, implying a good sieving behavior. The H_2/CO_2 separation factor of 11.67 could be achieved in the separation of 50%H_2/50%CO_2 mixture enabled this Si_3N_4 supported ZIF membrane to be a potential CO_2 adsorption and separation medium.

3.3. Membrane catalysis

Catalytic membrane reactors with the functions of reaction and separation were prepared and explored for broad applications [133,134]. Over the past several years, extensive efforts have focused on using the catalytic ceramic membranes to improve the methane conversion processes, combining air separation from the air and simultaneously high-temperature catalytic oxidation of methane to ethylene and ethane (C_2 products) or syngas ($CO+H_2$) in a single step, the schematic diagram of which was described in Fig. 9 [135,136]. The employing of the catalytic membrane reactors in methane conversion processes could prevent the formation of N_2 impurity component and NO_x environmental pollutants during the high-temperature reaction, circumvent flammability limits due to diffusion-limited operation,

reduce greatly the cost of gas compression in downstream processing, produce pure oxygen at small- and intermediate-scales [137,138]. In the C_2 production membrane reactor, methane and oxygen (air) feeds are separated by the (disk-shaped or tubular) membrane wall, and the reactions occur on one surface of the membrane involving surface oxygen supplied from the other surface. Ideally, no oxygen should be present in the methane side and react with reactant and product in the gas phase, thus, maximizing the selectivity for desired products. In the case of syngas production by partial oxidation of methane, the perovskite membrane serves as an oxygen distributor to provide optimum oxygen partial pressure in the axial direction of the reactor. For these applications, the membrane reactors should be tubular.
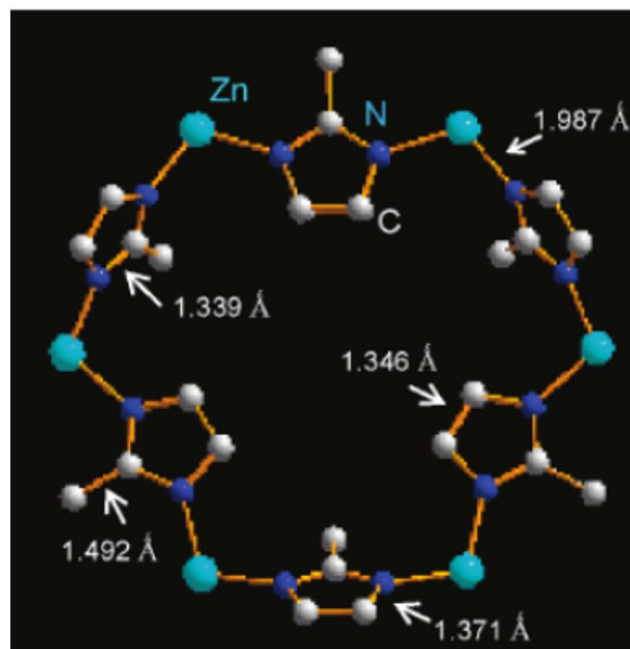
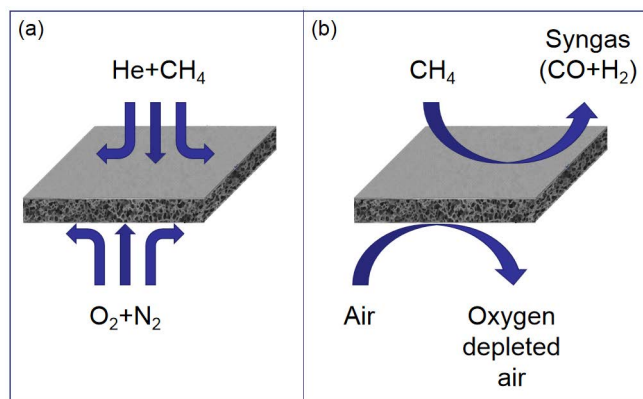

Fig. 8. The framework of ZIF-8.

Fig. 9. Illustration of ceramic membrane reactor for the oxidation of methane to (a) ethylene and ethane (C_2 products) and (b) syngas ($CO + H_2$).

Table 3
Literature derived from section 2 and section 3 and their comparison

Major raw material	Method	Layers	Sintering temperature (°C)	Average pore size (μm)	Porosity (%)	Application	Reference
Moroccan clay	Sintering/sol–gel	3	1,225	0.05	43	Dye wastewater treatment	[47]
IIT Guwahati clay	Sintering	1	900	4.58	38	Heavy metal removal	[48]
Kaolin + IIT Guwahati clay	Sintering/dipping	2	1,000	0.013	37	Heavy metal removal	[49]
Silty marls	Sintering/slip-casting	2	1,000	0.4	50	Tangential wastewater filtration	[50]
India Kaolin + zirconia	Sintering/depositing	3	900	1.3	-	Oil-water emulsion and bacteria separation	[52]
Mineral kyanite	Sintering	1	1500	1.06	60.71	Oil and bacteria separation	[54]
Zeolite	Sintering/dipping	3	850	0.54	56	Oily wastewaters treatment	[58]
Bentonite	Sintering	1	950	1.7	30	Discoloration of textile wastewater	[65]
Cordierite	Sintering	1	1380	8.66	36.2	Pre-treatment of strong alkali media and dust-containing hot gas	[70]
Apatite	Sintering/slip-casting	2	750	0.25	47	Turbidity, COD, germ, conductivity removal	[73]
Perovskite	Compression	1	–	–	–	Oxygen permeation	[78]
Pozzolan	Sintering/crossflow filtration	2	950	1.12	41.2	Turbidity rejection, COD retention	[79]
Coal fly ash	depositing	2	800	0.25	51	Turbidity rejection, COD retention	[80]
Rice husk ash	Phase inversion/sintering	1	1200	1.2	36.7	Heavy metal separation and adsorption	[92]
Clay + fly ash	Sintering	2	900	0.005	36.2	Phosphate treatment	[97]
Kaolin	Sintering	1	900	1.32	30	Heavy metal removal, bacteria rejection	[104]
Kaolin	Sintering	1	900	0.285	23.676	Juice clarification	[124]

Table 4
Cost of the ceramic membranes prepared from the cost effective raw materials

Major raw material	Method	Shape	Sintering temperature (°C)	Price ($ m^{-2})	Reference
Kaolin	Paste/sintering	Disc	850	130	[143]
Kaolin	Paste/sintering	Disc	900	220	[123]
Kaolin	Paste/sintering	Disc	900	61	[104]
Kaolin	Paste/sintering	Disc	900	78	[144]
Kaolin	Paste/sintering	Disc	950	172	[145]
Kaolin	Dry compaction	Tubular	850	332	[146]
Kaolin	Dry compaction	Disc	900	63	[147]
Kaolin	Casting/sintering	Disc	850	92	[148]
Kaolin	Extrusion/sintering	Tubular	1,100	70	[149]
Clay	Paste/sintering	Disc	1,000	100	[48]
Clay	Extrusion/sintering	Tubular	950	69	[150]
Clay	Paste/sintering/chitosan dip-coating	Disc	1,000	600	[49]
Clay	Paste/sintering/cellulose acetate dip-coating	Disc	1,000	100	[114]

The La based perovskite oxides are typical of mixed ionic and electronic-conducting ceramic membrane materials with very high oxygen semipermeability. The $La_{0.8}Sr_{0.2}Co_{0.6}Fe_{0.4}O_{3-\delta}$ (LSCF) membrane was synthesized by the coprecipitation method and introduced in the membrane reactor for oxidative coupling of methane (OCM) [139]. One side of the membrane was exposed to the O_2/N_2 mixture stream and the other side to the He/CH_4 mixture atmosphere. The surface catalytic property of LSCF membranes for OCM was demonstrated strongly depend on the oxygen permeation and consumption rates of the membrane surface exposed to the methane stream. At temperatures higher than 850°C, high ethylene and ethane (C_2) selectivity (70%–90%) and yield (10%–18%) were achieved with a feed ratio (He/CH_4) of 40–90.

For better visualization, the related literature derived from section 2 and section 3 have been listed in Table 3.

4. Membrane cost

In connection with the membrane preparation and its applications, cost evaluation is a competitive perspective to validate the viability of mineral-based and waste-based membranes compared to those commercial membranes. The membrane cost based on the cost-effective raw materials, as listed in Table 4, is varied significantly depending on the raw material, membrane shape, preparation method, sintering temperature, etc. since the manufacturing and shipment costs were supposed to be considered. Conventional polymeric membranes are available for industrial-scale operation cost around $50–200 m^{-2} [140]. However, often inorganic membranes are quoted to be at least 10 times expensive than the polymeric membranes and their cost is projected to be around $500–1,000 m^{-2} [141]. A α-alumina ceramic symmetric membrane tubes with 1,000–6,000 nm costs in a similar range of $500–1,000 m^{-2}, and stainless steel asymmetric membranes cost around $3,000 m^{-2} [142].

However, in the practical application, the membrane lifetime should be considered as well as membrane cost.

Even with the relatively high cost, the higher mechanical stability and the higher chemical stability resulting in a longer lifetime of the ceramic membrane [30–36]. Moreover, the ceramic membranes prepared from natural minerals and industrial wastes have been identified as an effective approach to further reduce the ceramic membrane cost, making the cost-effective ceramic membranes are well suited for challenging water purification processes.

5. Conclusions and future perspectives

It is generally believed to all that ceramic membrane has been broadly explored for wastewater treatment and resource recovery, such as treatment of colored wastewater, oil–water separation, produced water as well as recovery of the valuable component by concentration feed solution. Compared to the conventional starting material of ceramic membrane, several natural materials (clay, silty marls, kaolin, zeolite, bauxite, quartz sands, bentonite, cordierite, apatite, perovskite, etc.) and industrial wastes (coal fly ash, coal gangue, blast furnace slag, rice husk ash, pozzolan, etc.) in abundance needed lower firing temperature than metal oxide materials, especially emphasized the remarkable cost reduction of membrane fabrication. These low-cost ceramic membranes have been broadly applicable to a variety of applications of liquid treatment (removal of solid, dye, ion, heavy metal, oily wastewater treatment, juice clarification, seawater desalination, sterilization, etc.), gas separation (hydrogen separation, oxygen permeation, CO_2 adsorption and separation, etc.) and membrane catalysis. These natural minerals and industrial wastes based ceramic membranes were estimated to be cost-effective when compared with the conventional oxide ceramic membrane.

Together with the abundance and economic, the performance of the fabricated cost-effective ceramic membrane was thought to be the decisive characteristic for applications. However, the weakened mechanical strength, reduced operational temperature, as well as unmanageable pore size restricted the widespread applications. In the future, there

is still a large space for the performance improvement of these cost-effective ceramic membranes. We envision that this waste-to-resource approach will continuously create a more economically viable and environmentally sustainable strategy toward the management of waste and fabrication of high-performance ceramic membranes.

Acknowledgments

References

[1] D. Sugawara, K. Minoura, F. Imamura, Chapter 3 – Tsunamis and Tsunami Sedimentology, T. Shiki, Y. Tsuji, T. Yamazaki, K. Minoura, Eds., Tsunamiites, 2008, pp. 9–49.

[2] G.M.R. Vandenbossche, P. Van Oostveldt, J.P. Remon, A fluorescence method for the determination of the molecular weight cut-off of alginat-polylysine microcapsules, J. Pharm. Pharmacol., 43 (1991) 275–277.

[3] R.L. Stover, A.O. Fernández, J. Galtés, Permeate Recovery Rate Optimization at the Alicante Spain SWRO Plant, Proceedings of the International Desalination Association World Congress, Dubai, UAE, 2009.

[4] J. Campbell, Complete Casting Handbook: Metal Casting Processes, Metallurgy, Techniques and Design, Butterworth-Heinemann, 2015.

[5] B. Erzar, P. Forquin, An experimental method to determine the tensile strength of concrete at high rates of strain, Exp. Mech., 50 (2010) 941–955.

[6] K.S. Naveen, J.P. Singh, M. Viswambaran, R.K. Dhiman, Evaluation of flexural strength of resin interim restorations impregnated with various types of silane treated and untreated glass fibres, Med. J. Armed Forces India, 71 (2015) S293–S298.

[7] J.I. Mwasiagi, X.B. Huang, X.H. Wang, Performance of neural network algorithms during the prediction of yarn breaking elongation, Fibers Polym., 9 (2008) 80–86.

[8] J. Bhadra, A. Abdulkareem, N. Al-Thani, Chapter 6 – Nanotechnology in Decontamination, G.Z. Kyzas, A.C. Mitropoulos, Eds., Composite Nanoadsorbents: Micro and Nano Technologies, Elsevier, 2019, pp. 119–137.

[9] Y.H. Yuan, T.R. Lee, Contact Angle and Wetting Properties, G. Bracco, B. Holst, Eds., Surface Science Techniques, Springer, Berlin, Heidelberg, 2013, pp. 3–34.

[10] A. Luo, N. Lior, Study of advancement to higher temperature membrane distillation, Desalination, 419 (2017) 88–100.

[11] M.A. Uddin, H.P. Chan, Chapter 8 – Adhesive Technology for Photonics, M.O. Alam, C. Bailey, Eds., Advanced Adhesives in Electronics: Materials, Properties and Applications Woodhead Publishing Series in Electronic and Optical Materials, Woodhead Publishing, 2011.

[12] J.F. Briand, Marine antifouling laboratory bioassays: an overview of their diversity, Biofouling, 25 (2009) 297–311.

[13] I. Campos, M. Palomar, A. Amador, R. Ganem, J. Martinez, Evaluation of the corrosion resistance of iron boride coatings obtained by paste boriding process, Surf. Coat. Technol., 201 (2006) 2438–2442.

[14] M. Ulbricht, Advanced functional polymer membranes, Polymer, 47 (2006) 2217–2262.

[15] R.E. Kesting, The four tiers of structure in integrally skinned phase inversion membranes and their relevance to the various separation regimes, J. Appl. Polym. Sci., 41 (1990) 2739–2752.

[16] Y. Shimizu, Y.I. Okuno, K. Uryu, S. Ohtsubo, A. Watanabe, Filtration characteristics of hollow fiber microfiltration membranes used in membrane bioreactor for domestic wastewater treatment, Water Res., 30 (1996) 2385–2392.

[17] J. Cui, X. Zhang, H. Liu, S. Liu, K.L. Yeung, Preparation and application of zeolite/ceramic microfiltration membranes for treatment of oil contaminated water, J. Membr. Sci., 325 (2008) 420–426.

[18] L. Carneiro, I. dos Santos Sa, F. dos Santos Gomes, V.M. Matta, L.M.C. Cabral, Cold sterilization and clarification of pineapple juice by tangential microfiltration, Desalination, 148 (2002) 93–98.

[19] L. Yan, S. Hong, M.L. Li, Y.S. Li, Application of the Al_2O_3-PVDF nanocomposite tubular ultrafiltration (UF) membrane for oily wastewater treatment and its antifouling research, Sep. Purif. Technol., 66 (2009) 347–352.

[20] C. Mbareck, Q.T. Nguyen, O.T. Alaoui, D. Barillier, Elaboration, characterization and application of polysulfone and polyacrylic acid blends as ultrafiltration membranes for removal of some heavy metals from water, J. Hazard. Mater., 171 (2009) 93–101.

[21] S. Barredo-Damas, M.I. Alcaina-Miranda, M.I. Iborra-Clar, J.A. Mendoza-Roca, Application of tubular ceramic ultrafiltration membranes for the treatment of integrated textile wastewaters, Chem. Eng. J., 192 (2012) 211–218.

[22] A. Bhattacharya, P. Ghosh, Nanofiltration and reverse osmosis membranes: theory and application in separation of electrolytes, Rev. Chem. Eng., 20 (2004) 111–173.

[23] V. Kočanová, J. Cuhorka, L. Dušek, P. Mikulášek, Application of nanofiltration for removal of zinc from industrial wastewater, Desal. Water Treat., 75 (2017) 342–347.

[24] Y. Qing, L.S. Zhang, Y.Z. Li, Y.X. Pu, W.B. Zhu, Studies on the application of nanofiltration membranes to the treatment of pesticide wastewater, Ind. Water Treat., 3 (2009) 10.

[25] K.L. Tu, L.D. Nghiem, A.R. Chivas, Boron removal by reverse osmosis membranes in seawater desalination applications, Sep. Purif. Technol., 75 (2010) 87–101.

[26] J.H. Al-Rifai, H. Khabbaz, A.I. Schäfer, Removal of pharmaceuticals and endocrine disrupting compounds in a water recycling process using reverse osmosis systems, Sep. Purif. Technol., 77 (2011) 60–67.

[27] O.A. Bamaga, A. Yokochi, E.G. Beaudry, Application of forward osmosis in pretreatment of seawater for small reverse osmosis desalination units, Desal. Water Treat., 5 (2009) 183–191.

[28] K. Lutchmiah, L. Lauber, K. Roest, D.J.H. Harmsen, J.W. Post, L.C. Rietveld, J.B. van Lier, E.R. Cornelissen, Zwitterions as alternative draw solutions in forward osmosis for application in wastewater reclamation, J. Membr. Sci., 460 (2014) 82–90.

[29] N.K. Rastogi, Opportunities and challenges in application of forward osmosis in food processing, Crit. Rev. Food Sci. Nutr., 56 (2016) 266–291.

[30] H.K. Oh, S. Takizawa, S. Ohgaki, H. Katayama, K. Oguma, M.J. Yu, Removal of organics and viruses using hybrid ceramic MF system without draining PAC, Desalination, 202 (2007) 191–198.

[31] S.M. Samaei, S. Gato-Trinidad, A. Altaee, The application of pressure-driven ceramic membrane technology for the treatment of industrial wastewaters–a review, Sep. Purif. Technol., 200 (2018) 198–220.

[32] H. Ramlow, R.K.M. Ferreira, C. Marangoni, R.A.F. Machado, Ceramic membranes applied to membrane distillation: a comprehensive review, Int. J. Appl. Ceram. Technol., 16 (2019) 2161–2172.

[33] R.J. Ciora Jr., P.K.T. Liu, Ceramic membranes for environmental related applications, Fluid/Part. Sep. J., 15 (2003) 51–60.

[34] B. Hofs, S.G.J. Heijman, J.Z. Hamad, M.D. Kennedy, G. Amy, Ceramic Microfiltration with a Sub-Micron PAC Pre-Coat for Water Treatment, J.P.T. Melin, M. Dohmann, Eds., Aachener Tagung Wasser und Membranen, Vol. 8, Aachen, 2009, p. W12.

[35] B. van der Bruggen, C. Vandecasteele, T. van Gestel, W. Doyen, R. Leysen, A review of pressure-driven membrane processes in wastewater treatment and drinking water production, Environ. Prog., 22 (2003) 46–56.

[36] E.R. Cornelissen, B. Hofs, U. Muller, E.F. Beerendonk, S.G.J. Heijman, Direct and Hybrid Ceramic Microfiltration in Water Treatment, TECHNEAU: Safe Drinking Water from Source to Tap, IWA Publishing, Maastricht, 2009, pp. 83–97.

[37] K.A. DeFriend, M.R. Wiesner, A.R. Barron, Alumina and aluminate ultra-filtration membranes derived from alumina nanoparticles, J. Membr. Sci., 224 (2003) 11–28.

[38] Y. Yoshino, T. Suzuki, B.N. Nair, H. Taguchi, N. Itoh, Development of tubular substrates, silica based membranes and membrane modules for hydrogen separation at high temperature, J. Membr. Sci., 267 (2005) 8–17.

[39] J. Caro, Hierarchy in inorganic membranes, Chem. Soc. Rev., 45 (2016) 3468–3478.

[40] A. Majouli, S. Tahiri, S.A. Younssi, H. Loukili, A. Albizane, Elaboration of new tubular ceramic membrane from local moroccan perlite for microfiltration process. Application to treatment of industrial wastewaters, Ceram. Int., 38 (2012) 4295–4303.

[41] R.D. Colle, C.A. Fortulan, S.R. Fontes, Manufacture and characterization of ultra and microfiltration ceramic membranes by isostatic pressing, Ceram. Int., 37 (2011) 1161–1168.

[42] S. Masmoudi, R.B. Amar, A. Larbot, H.E. Feki, A.B. Salah, L. Cot, Elaboration of inorganic microfiltration membranes with hydroxyapatite applied to the treatment of wastewater from sea product industry, J. Membr. Sci., 247 (2005) 1–9.

[43] X. Wang, Z. Yang, C. Yu, L. Yin, C. Zhang, X. Gu, Preparation of T-type zeolite membranes using a dip-coating seeding suspension containing colloidal SiO_2, Microporous Mesoporous Mater., 197 (2014) 17–25.

[44] Z. Liu, G. Zhang, X. Dong, W. Jiang, W. Jin, N. Xu, Fabrication of asymmetric tubular mixed-conducting dense membranes by a combined spin-spraying and co-sintering process, J. Membr. Sci., 415–416 (2012) 313–319.

[45] A. Abdullayev, M.F. Bekheet, D.A.H. Hanaor, A. Gurlo, Materials and applications for low-cost ceramic membranes, Membranes, 9 (2019) 105.

[46] B.F. Jones, E. Galan, Reviews in Mineralogy, S.W. Bailey, P.H. Ribbe, Eds., Hydrous Phyllosilicates (Exclusive of Micas), Mineralogical Society of America, Washington, 1988, pp. 631–674.

[47] N. Saffaj, M. Persin, S.A. Younsi, A. Albizane, M. Cretin, A. Larbot, Elaboration and characterization of microfiltration and ultrafiltration membranes deposited on raw support prepared from natural Moroccan clay: application to filtration of solution containing dyes and salts, Appl. Clay Sci., 31 (2006) 110–119.

[48] S. Jana, M.K. Purkait, K. Mohanty, Preparation and characterization of low-cost ceramic microfiltration membranes for the removal of chromate from aqueous solutions, Appl. Clay Sci., 47 (2010) 317–324.

[49] S. Jana, A. Saikia, M.K. Purkait, K. Mohanty, Chitosan based ceramic ultrafiltration membrane: preparation, characterization and application to remove Hg(II) and As(III) using polymer enhanced ultrafiltration, Chem. Eng. J., 170 (2011) 209–219.

[50] S. Khemakhem, R.B. Amar, R.B. Hassen, A. Larbot, M. Medhioub, A.B. Salah, L. Cot, New ceramic membranes for tangential waste-water filtration, Desalination, 167 (2004) 19–22.

[51] S.K. Hubadillah, M.H.D. Othman, T. Matsuura, A.F. Ismail, M.A. Rahman, Z. Harun, J. Jaafar, M. Nomura, Fabrications and applications of low cost ceramic membrane from kaolin: a comprehensive review, Ceram. Int., 44 (2018) 4538–4560.

[52] D. Vasanth, G. Pugazhenthi, R. Uppaluri, Fabrication and properties of low cost ceramic microfiltration membranes for separation of oil and bacteria from its solution, J. Membr. Sci., 379 (2011) 154–163.

[53] N. Medjemem, A. Harabi, F. Bouzerara, L. Foughali, B. Boudaira, A. Guechi, N. Brihi, Elaboration and characterization of low cost ceramics microfiltration membranes applied to the sterilization of plant tissue culture media, J. Taiwan Inst. Chem. Eng., 59 (2016) 79–85.

[54] H. Guo, W. Li, F. Ye, Low-cost porous mullite ceramic membrane supports fabricated from kyanite by casting and reaction sintering, Ceram. Int., 42 (2016) 4819–4826.

[55] C.-Y. Bai, Y. Li, Z.-M. Liu, P.-W. Liu, X.-Y. Deng, J.-B. Li, J. Yang, Fabrication and properties of mullite-bonded porous SiC membrane supports using bauxite as aluminum source, Ceram. Int., 41 (2015) 4391–4400.

[56] L. Li, X. Dong, Y. Dong, L. Zhu, S.-J. You, Y.-F. Wang, Incorporation of zinc for fabrication of low-cost spinel-based composite ceramic membrane support to achieve its stabilization, J. Hazard. Mater., 287 (2015) 188–196.

[57] Q. Lü, X. Dong, Z. Zhu, Y. Dong, Environment-oriented low-cost porous mullite ceramic membrane supports fabricated from coal gangue and bauxite, J. Hazard. Mater., 533 (2014) 136–145.

[58] M. Abbasi, M. Mirfendereski, M. Nikbakht, M. Golshenas, T. Mohammadi, Performance study of mullite and mullite–alumina ceramic MF membranes for oily wastewaters treatment, Desalination, 259 (2010) 169–178.

[59] R.W. Broach, D. Jan, D.A. Lesch, S. Kulprathipanja, E. Roland, P. Kleinschmit, Zeolite, Ullmann's Encyclopedia of Industrial Chemistry, 1982.

[60] Y. Dong, S. Chen, X. Zhang, J. Yang, X. Liu, G. Meng, Fabrication and characterization of low cost tubular mineral-based ceramic membranes for micro-filtration from natural zeolite, J. Membr. Sci., 281 (2006) 592–599.

[61] Y. Dong, X. Feng, X. Feng, Y. Ding, X. Liu, G. Meng, Preparation of low-cost mullite ceramics from natural bauxite and industrial waste fly ash, J. Alloys Compd., 460 (2008) 599–606.

[62] O. Şan, C. Özgür, Fabrication of glassy ceramic membrane filters for filtration of spring water with clogging phenomena, J. Membr. Sci., 305 (2007) 169–175.

[63] A. Chakir, J. Bessiere, K.E. Kacemi, B. Marouf, A comparative study of the removal of trivalent chromium from aqueous solutions by bentonite and expanded perlite, J. Hazard. Mater., 95 (2002) 29–46.

[64] M. Roulia, A. Alexandros, A. Vassiliadis, Sorption characterization of a cationic dye retained by clays and perlite, Microporous Mesoporous Mater., 116 (2008) 732–740.

[65] A. Bouazizi, M. Breida, A. Karim, B. Achiou, M. Ouammou, J.I. Calvo, A. Aaddane, K. Khiat, S. Alami Younssi, Development of a new TiO_2 ultrafiltration membrane on flat ceramic support made from natural bentonite and micronized phosphate and applied for dye removal, Ceram. Int., 43 (2017) 1479–1487.

[66] C.M. Hung, Cordierite-supported Pt-Pd-Rh ternary composite for selective catalytic oxidation of ammonia, Powder Technol., 200 (2010) 78–83.

[67] D. Njoya, A. Elimbi, D. Fouejio, M. Hajjaji, Effects of two mixtures of kaolin-talc-bauxite and firing temperatures on the characteristics of cordierite-based ceramics, J. Build. Eng., 8 (2016) 99–106.

[68] N.E. Hipedinger, A.N. Scian, E.F. Aglietti, Magnesia-ammonium phosphate-bonded cordierite refractory castables: phase evolution on heating and mechanical properties, Cem. Concr. Res., 34 (2004) 157–164.

[69] X. Zhang, D. Fang, B. Lin, Y. Dong, G. Meng, X. Liu, Asymmetric porous cordierite hollow fiber membrane for microfiltration, J. Alloys Compd., 487 (2009) 631–638.

[70] Y. Dong, X. Feng, D. Dong, S. Wang, J. Yang, J. Gao, X. Liu, G. Meng, Elaboration and chemical corrosion resistance of tubular macro-porous cordierite ceramic membrane supports, J. Membr. Sci., 304 (2007) 65–75.

[71] G. Montel, G. Bonel, M. Heugheubaert, J.C. Trombe, C. Rey, New concepts in the composition, crystallisation and growth of the mineral component of calcified tissues, J. Cryst. Growth, 53 (1981) 74–99.

[72] J.R. Van Wazer, Phosphorus and its Compounds Chemistry, 1st ed., Interscience, New York, 1958.

[73] S. Masmoudi, A. Larbot, H. El Feki, R. Ben Amar, Elaboration and properties of new ceramic microfiltration membranes from natural and synthesised apatite, Desalination, 190 (2006) 89–103.

[74] J. Sunarso, S. Baumann, J.M. Serra, W.A. Meulenberg, S. Liu, Y.S. Lin, J.C. Diniz da Costa, Mixed ionic–electronic conducting (MIEC) ceramic-based membranes for oxygen separation, J. Membr. Sci., 320 (2008) 13–41.

[75] A. Burgraaf, L. Cot, Fundamentals of Inorganic Membrane Science and Technology, Elsevier, Amsterdam, 1996.

[76] P. Haworth, S. Smart, J. Glasscock, J.C. Diniz da Costa, Yttrium doped BSCF membranes for oxygen separation, Sep. Purif. Technol., 81 (2011) 88–93.

[77] J. Tong, W. Yang, B. Zhu, R. Cai, Investigation of ideal zirconium-doped perovskite-type ceramic membrane materials for oxygen separation, J. Membr. Sci., 203 (2002) 175–189.

[78] X. Chen, H. Liu, Y. Wei, J. Caro, H. Wang, A novel zincum-doped perovskite-type ceramic membrane for oxygen separation, J. Alloys Compd., 484 (2009) 386–389.

[79] B. Achiou, H. Elomari, A. Bouazizi, A. Karim, M. Ouammou, A. Albizane, J. Bennazha, S. Alami Younssi, I.E. El Amrani, Manufacturing of tubular ceramic microfiltration membrane based on natural pozzolan for pretreatment of seawater desalination, Desalination, 419 (2017) 181–187.

[80] I. Jedidi, S. Saïdi, S. Khemakhem, A. Larbot, N. Elloumi-Ammar, A. Fourati, A. Charfi, A. Ben Salaha, R. Ben Amar, Elaboration of new ceramic microfiltration membranes from mineral coal fly ash applied to waste water treatment, J. Hazard. Mater., 172 (2011) 152–158.

[81] E. Mulder, A mixture of fly ashes as road base construction material, Waste Manage., 16 (1996) 15–20.

[82] C. Palmonari, G. Nassetti, Evolution, Future Trends of Traditional Ceramics, American Ceramic Society Bulletin, 73 (1994) 42–46.

[83] M. Ilic, C. Cheeseman, C. Sollars, J. Knight, Mineralogy and microstructure of sintered lignite coal fly ash, Fuel, 82 (2003) 331–336.

[84] J. Liu, Y. Dong, X. Dong, S. Hampshire, L. Zhu, Z. Zhu, L. Li, Feasible recycling of industrial waste coal fly ash for preparation of anorthite-cordierite based porous ceramic membrane supports with addition of dolomite, J. Eur. Ceram. Soc., 36 (2016) 1059–1071.

[85] J. Fang, G. Qin, W. Wei, X. Zhao, L. Jiang, Elaboration of new ceramic membrane from spherical fly ash for microfiltration of rigid particle suspension and oil-in-water emulsion, Desalination, 311 (2013) 113–126.

[86] X. Querol, M. Izquierdo, E. Monfort, E. Alvarez, O. Font, T. Moreno, A. Alastuey, X. Zhuang, W. Lu, Y. Wang, Environmental characterization of burnt coal gangue banks at Yangquan, Shanxi Province, China, Int. J. Coal Geol., 75 (2008) 93–104.

[87] J.D.N. Pone, K.A.A. Hein, G.B. Stracher, H.J. Annegarn, R.B. Finkleman, D.R. Blake, J.K. McCormack, P. Schroeder, The spontaneous combustion of coal and its by-products in the Witbank and Sasolburg coalfields of South Africa, Int. J. Coal Geol., 72 (2007) 124–140.

[88] D.H. Yan, K.H. Karstensen, Q.F. Huang, Q. Wang, M.L. Cai, Coprocessing of industrial and hazardous wastes in cement kilns: a review of current status and future needs in China, Environ. Eng. Sci., 53 (2010) 37–45.

[89] C. Zhou, G. Liu, S. Wu, P.K.S. Lam, The environmental characteristics of usage of coal gangue in bricking-making: a case study at Huainan, China, Chemosphere, 95 (2014) 534–280.

[90] M. Yang, Z. Guo, Y. Deng, X. Xing, K. Qiu, J. Long, J. Li, Preparation of CaO-Al$_2$O$_3$-SiO$_2$ glass ceramics from coal gangue, Int. J. Miner. Process., 102 (2012) 112–115.

[91] F. Mohammadi, T. Mohammadi, Optimal conditions of porous ceramic membrane synthesis based on alkali activated blast furnace slag using Taguchi method, Ceram. Int., 43 (2017) 14369–14379.

[92] S.K. Hubadillah, M.H.D. Othman, Z. Harun, A.F. Ismail, M.A. Rahman, J. Jaafar, A novel green ceramic hollow fiber membrane (CHFM) derived from rice husk ash as combined adsorbent-separator for efficient heavy metals removal, Ceram. Int., 43 (2017) 4716–4720.

[93] P.X. Sheng, Y.P. Ting, J.P. Chen, L. Hong, Sorption of lead, copper, cadmium, zinc, and nickel by marine algal biomass: characterization of biosorptive capacity and investigation of mechanisms, J. Colloid Interface Sci., 535 (2004) 131–141.

[94] S. Zhou, A. Xue, Y. Zhang, X. Huang, M. Li, Y. Zhao, Y. Fan, W. Xing, Preparation of a new ceramic microfiltration membrane with a separation layer of attapulgite nanofibers, Mater. Lett., 143 (2015) 53–30.

[95] P.B. Belibi, M.M.G. Nguemtchouin, M. Rivallin, J. Ndi Nsami, J. Sieliechi, S. Cerneaux, M.B. Ngassoum, M. Cretin, Microfiltration ceramic membranes from local Cameroonian clay applicable to water treatment, Ceram. Int., 41 (2015) 2752–2759.

[96] X. Cheng, N. Li, M. Zhu, L. Zhang, Y. Deng, C. Deng, Positively charged microporous ceramic membrane for the removal of titan yellow through electrostatic adsorption, J. Environ. Sci., 44 (2016) 204–212.

[97] G. Wei, B. Fan, Y. Wei, S. Xu, Z. Zhao, N. Qiao, Preparation of a nano-scale ceramic membrane and its application in the medium-pressure boiler with phosphate treatment, Desalination, 322 (2013) 167–175.

[98] S. Mimoune, R.E. Belazzougui, F. Amrani, Purification of aqueous solutions of metal ions by ultrafiltration, Desalination, 217 (2007) 251–259.

[99] P. Cañizares, Á. Pérez, R. Camarillo, Recovery of heavy metals by means of ultrafiltration with water-soluble polymers: calculation of design parameters, Desalination, 144 (2002) 539–285.

[100] C.P. Nanseu-Njiki, S.R. Tchamango, P.C. Ngom, A. Darchen, E. Ngameni, Mercury (II) removal from water by electrocoagulation using aluminum and iron electrodes, J. Hazard. Mater., 168 (2009) 1430–1436.

[101] K.M. Hassan, T. Fukuhara, F.I. Hai, Q.H. Bari, K.M.S. Islam, Development of a bio-physicochemical technique for arsenic removal from groundwater, Desalination, 249 (2009) 224–229.

[102] I.A. Katsoyiannis, A.I. Zouboulis, Application of biological processes for the removal of arsenic from groundwaters, Water Res., 38 (2004) 17–26.

[103] Y. Zheng, A. Wang, Removal of heavy metals using polyvinyl alcohol semi-IPN poly(acrylic acid)/tourmaline composite optimized with response surface methodology, Chem. Eng. J., 162 (2010) 186–193.

[104] D. Vasanth, G. Pugazhenthi, R. Uppaluri, Biomass assisted microfiltration of chromium (VI) using Baker's yeast by ceramic membrane prepared from low cost raw materials, Desalination, 285 (2012) 239–244.

[105] C.S. Johnston, R.J. Morris, Eds., Oily Water Discharges. Regulatory, Technical and Scientific Considerations, Applied Science Publishers Ltd., London, 1980, p. 225.

[106] M. Stewart, K. Arnold, Crude Oil Treating Systems, M. Stewart, K. Arnold, Eds., Emulsions and Oil Treating Equipment: Selection, Sizing and Troubleshooting, Gulf Professional Publishing, Burlington, 2009, pp. 1–80.

[107] X.S. Yi, S.L. Yu, W.X. Shi, N. Sun, L.M. Jin, S. Wang, B. Zhang, C. Ma, L.P. Sun, The influence of important factors on ultrafiltration of oil/water emulsion using PVDF membrane modified by nano-sized TiO$_2$/Al$_2$O$_3$, Desalination, 281 (2011) 179–184.

[108] D. Wandera, S.R. Wickramasinghe, S.M. Husson, Modification and characterization of ultrafiltration membranes for treatment of produced water, J. Membr. Sci., 373 (2011) 178–188.

[109] P. Janknecht, A.D. Lopes, A.M. Mendes, Removal of industrial cutting oil from oil emulsions by polymeric ultra- and microfiltration membranes, Environ. Sci. Technol., 38 (2004) 4878–4883.

[110] K. Bensadok, M. Belkacem, G. Nezzal, Treatment of cutting oil/water emulsion by coupling coagulation and dissolved air flotation, Desalination, 206 (2007) 440–448.

[111] R.W. Baker, Research needs in the membrane separation industry: Looking back, looking forward, J. Membr. Sci., 362 (2010) 134–136.

[112] D. Zou, M. Qiu, X. Chen, E. Drioli, Y. Fan, One step co-sintering process for low-cost fly ash based ceramic microfiltration membrane in oil-in-water emulsion treatment, Sep. Purif. Technol., 210 (2019) 511–520.

[113] L. Zhu, X. Dong, M. Xu, F. Yang, M.D. Guiver, Y. Dong, Fabrication of mullite ceramic-supported carbon nanotube composite membranes with enhanced performance in direct separation of high-temperature emulsified oil droplets, J. Membr. Sci., 582 (2019) 140–150.

[114] P. Mittal, S. Jana, K. Mohanty, Synthesis of low-cost hydrophilic ceramic–polymeric composite membrane for treatment of oily wastewater, Desalination, 282 (2011) 54–62.

[115] M. Cheryan, Ultrafiltration and Microfiltration Handbook, CRC Press, 1998.

[116] B. Sarkar, S. DasGupta, S. De, Cross-flow electro-ultrafiltration of mosambi (*Citrus sinensis* (L.) *Osbeck*) juice, J. Food Eng., 89 (2008) 241–245.

[117] G. Capannelli, A. Bottino, S. Munari, D.G. Lister, G. Maschio, I. Becchi, The use of membrane processes in the clarification of orange and lemon juices, J. Food Eng., 21 (1994) 473–483.

[118] L. Espamer, C. Pagliero, A. Ochoa, J. Marchese, Clarification of lemon juice using membrane process, Desalination, 200 (2006) 565–567.

[119] A.F.G. Bailey, A.M. Barbe, P.A. Hogan, R.A. Johnson, J. Sheng, The effect of ultrafiltration on the subsequent concentration of grape juice by osmotic distillation, J. Membr. Sci., 164 (2000) 195–204.

[120] K.-S. Youn, J.-H. Hong, D.-H. Bae, S.-J. Kim, S.-D. Kim, Effective clarifying process of reconstituted apple juice using membrane filtration with filter-aid pretreatment, J. Membr. Sci., 228 (2004) 179–186.

[121] A. Cassano, E. Drioli, G. Galaverna, R. Marchelli, G.D. Silvestro, P. Cagnasso, Clarification and concentration of citrus and carrot juices by integrated membrane processes, J. Food Eng., 57 (2003) 153–163.

[122] C. Chhaya, P. Rai, G.C. Majumdar, S. Dasgupta, S. De, Clarification of watermelon (*Citrullus lanatus*) juice by microfiltration, J. Food Process Eng., 31 (2008) 768–782.

[123] A. Cassano, M. Marchio, E. Drioli, Clarification of blood orange juice by ultrafiltration: analyses of operating parameters, membrane fouling and juice quality, Desalination, 212 (2007) 15–53.

[124] B.K. Nandi, B. Das, R. Uppaluri, M.K. Purkait, Microfiltration of Mosambi juice using low cost ceramic membrane, J. Food Eng., 95 (2009) 597–605.

[125] S.T. Mitrouli, S.G. Yiantsios, A.J. Karabelas, M. Mitrakas, M. Føllesdal, P.A. Kjolseth, Pretreatment for desalination of seawater from an open intake by dual-media filtration: pilot testing and comparison of two different media, Desalination, 222 (2008) 24–37.

[126] S. Jeong, S.-J. Kim, L.H. Kim, M.S. Shin, S. Vigneswaran, T.V. Nguyen, I.S. Kim, Foulant analysis of a reverse osmosis membrane used pretreated seawater, J. Membr. Sci., 428 (2013) 434–444.

[127] S. Jeong, S.J. Kim, C.M. Kim, S. Vigneswaran, T.V. Nguyen, H.K. Shon, J. Kandasamy, I.S. Kim, A detailed organic matter characterization of pretreated seawater using low pressure microfiltration hybrid systems, J. Membr. Sci., 428 (2013) 290–300.

[128] M.A. Vetten, C.S. Yah, T. Singh, M. Gulumian, Challenges facing sterilization and depyrogenation of nanoparticles: effects on structural stability and biomedical applications, Nanomed. Nanotechnol. Biol. Med., 10 (2014) 1391–1399.

[129] Y.W. Cong, W. Fang, W. Tao, L.Y. Xing, R.B. Yong, F.O. Kengara, L.B. Zeng, X. Jiang, Effects of autoclaving and mercuric chloride sterilization on PAHs dissipation in a two-liquid-phase soil slurry, Pedosphere, 21 (2011) 56–64.

[130] Y. Shi, L. Xu, D. Gong, J. Lu, Effects of sterilization treatments on the analysis of TOC in water samples, J. Environ. Sci., 22 (2010) 789–795.

[131] A. Kumar, X. Yuan, A.K. Sahu, J. Dewulf, S.J. Ergas, H.V. Langenhove, A hollow fiber membrane photo-bioreactor for CO_2 sequestration from combustion gas coupled with wastewater treatment: a process engineering approach, J. Chem. Technol. Biotechnol., 85 (2010) 387–394.

[132] J.-W. Wang, N.-X. Li, Z.-R. Li, J.-R. Wang, X. Xu, C.-S. Chen, Preparation and gas separation properties of Zeolitic imidazolate frameworks-8 (ZIF-8) membranes supported on silicon nitride ceramic hollow fibers, Ceram. Int., 42 (2016) 8949–8954.

[133] H.W.J.P. Neomagus, G. Saracco, G.F. Versteeg, A fixed bed barrier reactor with separate feed of reactants, Chem. Eng. Commun., 184 (2001) 49–69.

[134] M.P. Pina, M. Menendez, J. Santamaría, The Knudsen-diffusion catalytic membrane reactor: an efficient contactor for the combustion of volatile organic compounds, Appl. Catal., B, 11 (1996) L19–53.

[135] M. Schwartz, J.H. White, A.F. Sammells, Catalytic Membrane Reactor with Two Component Three-Dimensional Catalysis, International Patent WO 99/21649, 1999.

[136] U. Balachandran, M.S. Kleefisch, T.P. Kobylinski, S.L. Morissette, S. Pei, Oxygen Ion-Conducting Dense Membranes, WO 94/24065, 1994.

[137] N. Itoh, M.A. Sanchez, W.C. Xu, K. Haraya, M. Hongo, Application of a membrane reactor system to thermal decomposition of CO_2, J. Membr. Sci., 77 (1993) 245–253.

[138] Y. Teraoka, Y. Matsumura, K. Asakura, S. Kagawa, Application of mixed conductive La-Sr-Co-Fe perovskites to NOx removal membrane reactors, Solid State Ionics, 99 (1999) 131–138.

[139] Y. Zeng, Y.S. Lin, S.L. Swartz, Perovskite-type ceramic membrane: synthesis, oxygen permeation and membrane reactor performance for oxidative coupling of methane, J. Membr. Sci., 150 (1998) 87–98.

[140] B.D. Bhide, S.A. Stern, A new evaluation of membrane processes for the oxygen-enrichment of air. I. Identification of optimum operating conditions and process configuration, J. Membr. Sci., 62 (1991) 13–35.

[141] W.J. Koros, R. Mahajan, Pushing the limits on possibilities for large scale gas separation: which strategies?, J. Membr. Sci., 175 (2000) 181–196.

[142] Mott Metallurgical Corporation, USA, 2007. Available at: http://www.mottcorp.com.

[143] B.K. Nandi, R. Uppaluri, M.K. Purkait, Preparation and characterization of low cost ceramic membranes for micro-filtration applications, Appl. Clay Sci., 42 (2008) 102–110.

[144] S. Emani, R. Uppaluri, M.K. Purkait, Preparation and characterization of low cost ceramic membranes for mosambi juice clarification, Desalination, 317 (2013) 32–40.

[145] B. Ghosh, M.K. Sinha, M.K. Purkait, A comparative analysis of low-cost ceramic membrane preparation for effective fluoride removal using hybrid technique, Desalination, 353 (2013) 2–13.

[146] S. Bose, C. Das, Role of binder and preparation pressure in tubular ceramic membrane processing: design and optimization study using response surface methodology (RSM), Ind. Eng. Chem. Res., 53 (2014) 12319–12329.

[147] S. Emani, R. Uppaluri, M.K. Purkait, Cross flow microfiltration of oil-water emulsions using kaolin based low cost ceramic membranes, Desalination, 341 (2014) 61–71.

[148] B. Das, B. Chakrabarty, P. Barkakati, Preparation and characterization of novel ceramic membranes for micro-filtration applications, Ceram. Int., 42 (2016) 14326–14333.

[149] Y. Rasouli, M. Abbasi, S.A. Hashemifard, Investigation of in-line coagulation-MF hybrid process for oily wastewater treatment by using novel ceramic membranes, J. Cleaner Prod., 161 (2017) 545–559.

[150] R.V. Kumar, L. Goswami, K. Pakshirajan, G. Pugazhenthi, Dairy wastewater treatment using a novel low cost tubular ceramic membrane and membrane fouling mechanism using pore blocking models, J. Water Process Eng., 13 (2016) 168–175.